

# Scaling Analysis of Fluctuating Strength Function

HIROKAZU AIBA

*Koka Women's College, 38 Kadono-cho Nishikyogoku, Ukyo-ku, 615 Kyoto, Japan*

and

MASAYUKI MATSUO

*Yukawa Institute for Theoretical Physics, Kyoto University, 601-01 Kyoto, Japan*

## ABSTRACT

We propose a new method to analyze fluctuations in the strength function phenomena in highly excited nuclei. Extending the method of multifractal analysis to the cases where the strength fluctuations do not obey power scaling laws, we introduce a new measure of fluctuation, called the local scaling dimension, which characterizes scaling behavior of the strength fluctuation as a function of energy bin width subdividing the strength function. We discuss properties of the new measure by applying it to a model system which simulates the doorway damping mechanism of giant resonances. It is found that the local scaling dimension characterizes well fluctuations and their energy scales of fine structures in the strength function associated with the damped collective motions.

## I. Introduction

Collective or single-particle modes of excitation which have high excitation energies usually become damped motions due to coupling with background compound states with high level density. Strengths of exciting such modes form a broad peak (when plotted as a function of the excitation energy of a nucleus) which are spread over an interval of excitation energy. A typical example is the giant resonances which have a damping width of MeV order while the resonance energy is several to a few tens MeV depending on quantum numbers and nuclear masses [1,2]. Strength distribution plotted as a function of the excitation energy is called strength function. The strength function usually shows a smooth profile such as Lorentzian shape, but it also exhibits fluctuations called fine structures when the strength function is studied in high resolution experiments [2–6].

An important origin of the damping of the giant resonances in heavy nuclei is the doorway coupling [1]. The collectivity of the excitation mode is described well in terms of a coherent superposition of 1p-1h excitations, as often prescribed by the RPA models. On the other hand, the damping of the mode is caused by (besides the particle escaping whose effect is small in heavy nuclei) coupling to other kinds of excitation modes such as 2p-2h excitations or 1p-1h plus low-lying vibrational modes, which are called doorway states. Although the doorway states couple further with more complicated states, e.g. many-particle many-hole states and have their own spreading width, the total damping width of the giant resonances is explained reasonably well by the doorway coupling [1]. It is argued that the doorway states influence also the fine structure of the strength distribution [5,6]. However, relation between the doorway states and the fine structures remains to be understood since it would depend on the spreading of doorway states into more complicated states, which is not very well known.

If we look at the strength function with the finest energy scale dissolving individual energy eigenstates by assuming small particle escaping, another mechanism of the strength fluctuation is expected to emerge. Because of the chaotic nature of the compound states at the high excitation energy, strengths associated with individual eigenstates would show statistical fluctuation following the Porter-Thomas distribution [7,8]. When the particle escaping width is larger than mean level spacing so that individual level peaks overlap, the Ericson fluctuation emerges [8–10]. However it is natural to expect that these statistical behaviors based on the random matrix theories [8,11–13] govern the strength fluctuation only at small energy scales. One should rather expect that the strength function associated with the damping of giant resonances involves different kinds of fluctuations coexisting at different energy scales. (Note also there exists an argument that experimental fine structures of particle decay strength distribution under a certain situation resembles large fluctuations in simulated spectra generated solely on the basis of the statistical Porter-Thomas fluctuation, known as the pandemonium [3,14]. Although this is another possible origin of the fine structures, the property of the statistical fluctuation should depend on the level density of compound states under discussion). Thus it is important to analyze the fluctuations of strength function in connection with the energy scales of the fluctuation.

In this paper, we propose a new method to perform such a fluctuation analysis of the strength functions. With this method we characterize the strength fluctuation with focus on its scaling behavior by taking a similar approach widely adopted to analyze fluctuation phenomena having self-similar multifractal structure [15–17]. The multifractal fluctuations accompany a characteristic scaling property obeying the power laws, and they are found in various kinds of chaotic classical dynamical systems [15–17]. Furthermore multifractal fluctuations in quantum wave functions are found recently for electrons in disordered matter [18–20]. The idea is also applied to the strength function fluctuations [21,22], and an approximate power scaling is found in a shell model calculation of the giant dipole resonances [22]. In contrast to these multifractal analyses, however, we consider in this paper more general situations where the fluctuation does not necessarily follow the scaling laws, and we rather try to characterize the scaling behavior which may be dependent on the energy scales due to different coexisting fluctuation mechanisms. For this purpose, we introduce a new measure of fluctuation by extending the generalized fractal dimension [23,24] used in the standard multifractal analysis. The new measure, which we call the local scaling dimension, characterizes the scaling property as a function of the energy scale of fluctuation. With use of simple examples, we will demonstrate in this paper how the local scaling dimension carries information on the dynamics of the damping process.

For the analysis of the strength fluctuations, the autocorrelation function has been used widely as a measure of fluctuation in various contexts. It was applied for example to analyze the Ericson fluctuation in compound nuclear reactions to derive the particle decay width [8,9], and also to the strength of giant resonances and the decay particle spectra [3,5]. The autocorrelation function and its Fourier transform is also used to characterize energy level fluctuations in the random matrix theories and chaotic quantal systems [25–28]. We will show that the present approach and the autocorrelation analysis are related to each other and that the local scaling analysis can be used to reveal the energy scales involved in the strength fluctuation.

The present method treats in a single framework strength fluctuations in wide range of the energy scale, covering the statistical fluctuations at the finest scale around the level spacing order as well as those associated with the doorway states at the larger scale. In the present paper, therefore, we use the word fine structure to denote all kinds

of strength fluctuations including the doorway fluctuations, which are sometimes called the intermediate structures in the literature.

The paper is organized as follows. In section II, we describe the formalism of the fluctuation analysis and introduce the local scaling dimension. In addition, relation to the autocorrelation function is clarified. In section III, employing a schematic model which simulates the doorway damping mechanism of giant resonance, we discuss in detail how the local scaling dimension characterizes fluctuations in the model strength function. In particular, an emphasis is put on the relation between the profile of the local scaling dimension and the energy scales involved in the doorway damping process. Finally, section IV is devoted to conclusions.

## II. Scaling Analysis of Strength Function

### A. Local Scaling Dimension

The strength function is expressed as [29]

$$S(E) = \sum_i S_i \delta(E - E_i + E_0), \quad (1)$$

for exciting the nucleus with excitation energy  $E$  by a probe which excite a mode under consideration if we neglect the coupling to continuum states of escaping particles and experimental resolutions for simplicity. Here  $E_i$  and  $E_0$  are the energy of discrete levels and the ground state energy of the whole nuclear many-body Hamiltonian, respectively, and  $S_i$  denotes the strength of exciting the  $i$ -th energy level. Let us assume strengths are normalized as  $\sum_i S_i = 1$ .

By smoothing the strength function with respect to the excitation energy  $E$  with a sufficiently large smoothing energy width, or by putting the strengths into energy bins with large bin width, a smooth profile (e.g. a Lorentzian shape) will show up. If small smoothing width or bin width is used, resultant distribution will exhibit fluctuation associated with fine structures of the original strength function. Thus the fluctuation of the strength function generally depends on the energy scale with which one measures. To evaluate the scale dependent fluctuation, we apply the method described below. It is an extension of the scaling analysis widely used to characterize multifractal structures [15–17].

Let us consider binned distribution of the strength function  $S(E)$  by dividing whole energy interval under consideration into  $L$  bins with length  $\epsilon$ . Strength contained in  $n$ -th bin is denoted by  $p_n$ ,

$$p_n \equiv \sum_{i \in n\text{-th bin}} S_i. \quad (2)$$

To characterize the fluctuation of the binned strength distribution  $\{p_n\}$ , moments of the distribution are introduced. This leads to the so-called partition function  $\chi_m(\epsilon)$  defined by

$$\chi_m(\epsilon) \equiv \sum_{n=1}^L p_n^m = L \langle p_n^m \rangle. \quad (3)$$

For completeness of the definition, we need to introduce an average of  $\chi_m(\epsilon)$  with respect to the bin boundary. This is because there is still arbitrariness in Eq.(3) concerning how the boundaries of bins are chosen even if the bin width  $\epsilon$  is fixed. To overcome this uncertainty, we make an average over different choices of the bin boundaries. When the average is done with sufficiently large numbers of choices so that the boundaries cover densely the energy axis, the averaged partition function becomes independent of the boundaries.

It is of special interest if the partition function has a scaling property. If we consider a trivial case where the strength is uniformly distributed with no fluctuation, i.e.,  $p_n = \text{const} = 1/L \propto \epsilon$  for all  $L$  and  $\epsilon$ , then a power law scaling  $\chi_m(\epsilon) \propto \epsilon^{(m-1)}$  holds for  $\chi_m(\epsilon)$  with respect to the bin width  $\epsilon$ . When the fluctuation is present, the partition function generally deviates from this limit. An extreme case of large fluctuation is the situation where the strength is concentrated in a single energy level. In this case the partition function becomes constant  $\chi_m(\epsilon) = 1$  for any value of  $\epsilon$  since the binned strength is then  $p_n = 1$  for only one bin, and  $p_{n'} = 0$  for the others. In other words the partition function  $\chi_m(\epsilon)$  scales with zero power. If the fluctuation shows a fractal structure, i.e., it has a self-similar structure against the change of the scale, the partition function shows a power scaling with power different from the trivial cases, like

$$\chi_m(\epsilon) \propto \epsilon^{D_m^{\text{fractal}}(m-1)}, \quad (4)$$

or equivalently a linear scaling between  $\log \chi_m(\epsilon)$  and  $\log \epsilon$ ,

$$\log \chi_m(\epsilon) \approx (m - 1)D_m^{\text{fractal}} \log \epsilon. \quad (5)$$

The scaling coefficient  $D_m^{\text{fractal}}$  called the generalized fractal dimension characterizes the multifractal [23,24]. The trivial case of uniform distribution corresponds to  $D_m^{\text{fractal}} = 1$ , implying a one dimensional uniform object in the  $E$  axis. The case of the single sharp peak corresponds to  $D_m^{\text{fractal}} = 0$  since it is just a dot (zero dimensional object).

It should be noted however that the partition function does not follow the power scaling law in general. The fluctuation of the binned strength may change when we change the bin width. This will happen when the strength function contains fluctuations having specific energy scales. For the case of the damping of giant resonance, fluctuation may reflect the doorway states such as 2p-2h configurations, for which their spreading width could be one of the energy scales involved. Also, when we look at very small energy scale comparable with average level spacing, strength fluctuation associated with individual energy levels may emerge. Therefore, it is more useful to analyze “how the partition function scales for different energy scales” than to seek the power scaling property. For this purpose, we introduce an extension of the generalized fractal dimension by defining the scaling coefficients as local linear coefficients of  $\log \chi_m(\epsilon)$  vs.  $\log \epsilon$  at each energy scale  $\epsilon$ , or equivalently defining by

$$D_m(\epsilon) \equiv \frac{1}{m - 1} \frac{\partial \log \chi_m(\epsilon)}{\partial \log \epsilon}. \quad (6)$$

We call this quantity the local scaling dimension since it is defined at each energy scale  $\epsilon$  and this is a function of  $\epsilon$ . Note also that if the local scaling dimension  $D_m(\epsilon)$  is constant over a long interval of the energy scale  $\epsilon$ , it implies presence of the multifractal structure of the strength fluctuation. In this case the local scaling dimension reduces to the standard generalized fractal dimension  $D_m^{\text{fractal}}$  defined by Eq. (5).

In actual calculation of the local scaling dimension, we define it by means of finite difference under the change of a factor 2,

$$D_m(\sqrt{2}\epsilon) = \frac{1}{m - 1} \frac{\log \chi_m(2\epsilon) - \log \chi_m(\epsilon)}{\log 2}, \quad (7)$$

rather than the derivative in Eq. (6). Using the finite difference, the calculation is very simple for all the moments. The local scaling dimension  $D_2(\epsilon)$  defined by the derivative has an exact form (34) expressed in terms of the individual energy levels  $E_i$  and associated strengths  $S_i$ , as given in Appendix A. However, exact calculation with use of Eqs. (6) and (30) is more complicated than the calculation using the finite difference (7) except for the second moment local scaling dimension  $D_2(\epsilon)$ . Note also that the finite difference gives an effective smoothing. We will discuss difference between the two definitions in Sec. III B.

## B. Schematic Examples

Let us illustrate how the local scaling dimension carries information on the fluctuation of strength function by using some schematic examples.

### 1. Lorentzian

As the first example, we consider the Lorentzian distribution

$$S(E) = \frac{1}{2\pi} \frac{\Gamma}{E^2 + \Gamma^2/4}. \quad (8)$$

This represents a typical peak profile associated with many kinds of damping processes. The Lorentzian distribution shows a smooth variation of the strength centered around the peak. Discreteness of the energy levels is neglected. Note that the Lorentzian distribution has one characteristic energy scale which is the FWHM of the distribution,  $\Gamma$ . The local scaling dimension  $D_m(\epsilon)$  associated with the Lorentzian is shown in Fig.1 as a function of the binning energy scale  $\epsilon$ . When the bin width  $\epsilon$  is smaller than  $\Gamma$ , the local scaling dimension  $D_m(\epsilon)$  takes the value close to 1, while  $D_m(\epsilon) \sim 0$  for  $\epsilon$  much larger than  $\Gamma$ . For  $\epsilon$  around  $\Gamma$ ,  $D_m(\epsilon)$  decreases sharply with increasing  $\epsilon$ . This behavior arises because continuous and smooth aspect of the Lorentzian distribution is dominantly measured by the scaling analysis using small bin width  $\epsilon \ll \Gamma$ , and the local scaling dimension goes to the limit of uniform distribution  $D_m(\epsilon) = 1$ . With large bin width  $\epsilon \gg \Gamma$ , most of strength is concentrated in a single bin, thus the local scaling dimension reaches to the sharp peak limit  $D_m(\epsilon) = 0$ . With the bin width  $\epsilon$  being the same order of the width  $\Gamma$  of the Lorentzian, a transition between the two limits occurs. Thus the profile of  $D_m(\epsilon)$  relates to the characteristic energy scale  $\Gamma$  of the Lorentzian. In fact the value of  $\epsilon$  where  $D_m(\epsilon)$  decreases most steeply corresponds well to  $\Gamma$  as seen in Fig. 1.

## 2. GOE strength fluctuation

If we distinguish the strengths associated with individual energy levels of highly excited nucleus, the strengths fluctuate from level to level on top of a smooth profile of strength distribution. The level-by-level fluctuation originates from the chaotic nature of excited nuclei and is known to follow generic statistical rules described by the random matrix theory of the Gaussian orthogonal ensemble (GOE) [8,11–13]. Let us characterize the GOE strength fluctuation by means of the scaling analysis.

When the strength fluctuation is described by the GOE, the strengths  $S_i$  for individual states fluctuate independently and their statistics follows the Porter-Thomas distribution [7,8] at large  $N_{\text{tot}}$  limit ( $N_{\text{tot}}$  being the dimension of the random matrix). The distribution of energy levels  $E_i$  follows a semi-circle level density in average, and the position of the individual energy levels fluctuates locally around the average. We treat here only the strength fluctuation by neglecting effects both of the average level distribution and of local energy level fluctuations. Namely we assume the uniform distribution of the energy levels. As discussed in Appendix B, influence of the local energy level fluctuation on the local scaling dimension is small due to the spectral rigidity of the GOE energy levels. In this treatment, the energy levels are chosen to be equally spaced:  $E_i = id$  ( $i = 1, 2, \dots, N_{\text{tot}}$ ), where  $d$  is the level spacing. The local scaling dimension is then given by

$$D_m(l) = \frac{1}{m-1} \sum_{i=1}^{m-1} \frac{l}{l+2i}, \quad (9)$$

where  $l \equiv \epsilon/d$  (the bin width measured in the unit of the level spacing  $d$ ) is used as the scaling parameter. We give its derivation in Appendix B.

An example of the GOE strength function is shown in Fig. 2(a). The strengths of individual states fluctuate strongly, i.e., there exist levels which have as large strength as factor tens of the average value of strength. This is because the Porter-Thomas distribution is a distribution with large skewness. Because of the strength fluctuation, the binned strengths also fluctuate when the bin width  $\epsilon$  is not very large compared with the level spacing  $d$ . The fluctuation of the binned strength  $\{p_n\}$  decreases as  $\epsilon$  increases since the binning operates as an averaging over levels included in bins.

The local scaling dimension  $D_m(l)$ , Eq. (9), is plotted in Fig. 2(b), which shows how fluctuation of the binned strength distribution changes as the energy scale (bin width)  $\epsilon$  changes. When we use the bins whose width is comparable with the level spacing ( $l \lesssim 10$ ), the binned distribution shows many spiky peaks caused by large  $S_i$  components. This leads to small values of  $D_m(\epsilon)$ . The fluctuation of the binned distribution is still large for the bin width of order of ten level spacings ( $l \sim 10^1$ ), where  $D_m(\epsilon)$  deviate significantly from the uniform limit  $D_m(\epsilon) = 1$ . It is washed out mostly only with large bin width of order of  $100d$ , where  $D_m(\epsilon) \approx 1$  is realized. It is also noted that the local scaling dimension  $D_m(\epsilon)$  for the higher moment (larger  $m$ ) takes significantly smaller values compared with the second moment ( $D_2(\epsilon)$ ) especially for the small bin widths  $l \lesssim 10^1$ . Since taking the higher moment emphasizes large components of the binned distribution  $\{p_n\}$ , the local scaling dimension  $D_m(\epsilon)$  for higher  $m$  reflects scaling property of those components. Small value of  $D_m(\epsilon)$  for large  $m$  indicates that the large components are distributed sparsely along the  $E$  axis, reflecting the spiky distribution of the GOE strength.

We evaluated also the local scaling dimension  $D_m(\epsilon)$  based on the finite difference definition, both by using the analytic evaluation Eq. (38) and by using numerical evaluation adopting 60 realizations of GOE. They give essentially the same curves as the those plotted in Fig. 2(b) based on Eq. (9), and the difference is almost invisible in this plotting scale.

When we include the energy level fluctuation, the local scaling dimensions is affected for small bin width  $\epsilon$  comparable to the level spacing. However, the effect is not very large and becomes negligible for  $\epsilon > 10d$ , as discussed in Appendix B.

## 3. Poisson fluctuation

As the third example, we consider the Poisson fluctuation. If we consider experimental spectra where events are counted in channels which corresponds to excitation energy bins, there always exists fluctuation in the spectra that originates from the counting statistics. Even if the strength distribution is completely uniform, counts in bins fluctuate statistically obeying the Poisson distribution. Relating the normalized ‘strength’  $p_n$  to the counts  $\{r_n\}$  in bins by  $p_n = r_n/N$  ( $N$  being the total counts), the partition function  $\chi_m$  is expressed in terms of the  $m$ -th moment of the Poisson distribution. Using the average number of counts  $l = \langle r_n \rangle$  as the scale of the bin width, the local scaling dimension  $D_m$  is given by

$$\begin{aligned}
D_m(l) &= \frac{1}{(m-1)} \frac{d \log(\langle r_n^m \rangle / l)}{d \log l} \\
&= \frac{l}{l+1}, \frac{l^2 + \frac{3}{2}l}{l^2 + 3l + 1}, \frac{l^3 + 4l^2 + \frac{7}{3}l}{l^3 + 6l^2 + 7l + 1}, \frac{l^4 + \frac{15}{2}l^3 + \frac{25}{2}l^2 + \frac{15}{4}l}{l^4 + 10l^3 + 25l^2 + 15l + 1} \quad (m = 2, 3, 4, 5).
\end{aligned} \tag{10}$$

The local scaling dimension takes the value significantly smaller than one for small  $l$  ( $l \lesssim 10$ ). It monotonically increases with increasing  $l$  and approaches to one. The behavior is similar to that of the GOE strength fluctuation, Fig.2(b), but the values of  $D_m$  for the Poisson fluctuation is closer to  $D_m = 1$  than the GOE fluctuation since the fluctuation associated with the Poisson distribution is smaller than the GOE fluctuation.

Expression (10) indicates that effects of the counting statistics diminish for  $l$  larger than several tens for which the uniform limit  $D_m \approx 1$  is almost achieved. We neglect the counting statistics in the other part of this paper.

### C. Relation to Autocorrelation Analysis

One often uses the autocorrelation function to characterize fluctuations of the strength function. The autocorrelation function for the strength function, defined by

$$C_2(\epsilon) \equiv \int S(E)S(E + \epsilon)dE, \tag{11}$$

$$= \sum_{i,j} S_i S_j \delta(\epsilon - E_j + E_i), \tag{12}$$

quantifies the fluctuation correlation as a function of the displacement energy  $\epsilon$ . Dependence of  $C_2(\epsilon)$  on the displacement energy  $\epsilon$  reveals the characteristic energy scale involved in the strength fluctuations. Since the local scaling dimension has a similar property as discussed above, one may expect relation between the autocorrelation function and the local scaling dimension. In fact, we can prove that  $C_2(\epsilon)$  is related to the partition function  $\chi_2(\epsilon)$  and the local scaling dimension  $D_2(\epsilon)$  for the second moment.

To this end, we introduce an integral function of  $C_2(\epsilon)$  by

$$B_2(\epsilon) \equiv \int_{-\epsilon}^{\epsilon} C_2(\epsilon')d\epsilon' = \sum_{ij} S_i S_j \theta(\epsilon - |E_i - E_j|). \tag{13}$$

Comparing Eq. (13) with the closed form expression Eq. (33) for the partition function, we find an equation

$$(1 + \epsilon \frac{d}{d\epsilon})\chi_2(\epsilon) = B_2(\epsilon). \tag{14}$$

Thus, the partition function is expressed as

$$\chi_2(\epsilon) = \frac{1}{\epsilon} \int_0^{\epsilon} B_2(\epsilon')d\epsilon', \tag{15}$$

in terms of the integral of  $B_2(\epsilon)$ .

Using this expression for Eq. (6), the local scaling dimension  $D_2(\epsilon)$  is written as

$$D_2(\epsilon) = \frac{B_2(\epsilon) - \chi_2(\epsilon)}{\chi_2(\epsilon)}, \tag{16}$$

which is expressed in terms of the integral  $B_2(\epsilon)$  and the double integral  $\chi_2(\epsilon)$  of the autocorrelation function  $C_2(\epsilon)$ .

The close connection between the autocorrelation function  $C_2(\epsilon)$  and the local scaling dimension  $D_2(\epsilon)$  can be seen easily for the case of the Lorentzian distribution. For the Lorentzian distribution, the autocorrelation function  $C_2(\epsilon) = \frac{1}{\pi} \frac{\Gamma}{\Gamma^2 + \epsilon^2}$  decreases monotonically with increasing  $\epsilon$  and its value changes most steeply around  $\epsilon \sim \Gamma$ , where  $\Gamma$  is the FWHM of the Lorentzian strength distribution. On the other hand, the local scaling dimension  $D_2(\epsilon)$  is given with use of Eq. (16) by

$$D_2(\epsilon) = \frac{\frac{\Gamma}{2\epsilon} \log((\epsilon/\Gamma)^2 + 1)}{\tan^{-1} \frac{\epsilon}{\Gamma} - \frac{\Gamma}{2\epsilon} \log((\epsilon/\Gamma)^2 + 1)}. \tag{17}$$

This function also decreases monotonically from  $D_2 = 1$  at  $\epsilon = 0$  with increasing  $\epsilon$ . The point of its steepest slope,  $\epsilon = 0.80\Gamma$ , (or  $\epsilon = 1.8\Gamma$  when plotted as a function of  $\log \epsilon$ ) corresponds well to the FWHM of the Lorentzian. This correspondence holds also for the local scaling dimensions  $D_m$  of higher moments as seen in the previous subsection.

There are two figures of merit for the use of the scaling analysis in comparison with the autocorrelation analysis. Firstly, the local scaling dimension  $D_m(\epsilon)$  has smooth  $\epsilon$  dependence while the autocorrelation function  $C_2(\epsilon)$  is a sum of the delta functions (if we do not include any smoothing procedure). This difference can be seen in Eq. (16) where the  $D_2(\epsilon)$  is expressed in terms of the integral functions of  $C_2(\epsilon)$ . Secondly, the local scaling dimensions  $D_m(\epsilon)$  for  $m > 2$  carry information on the higher moments of strength fluctuation.

### III. Analysis of Doorway Damping Model

In the following we shall discuss fluctuations of the strength function which is associated with damping phenomena of a specific state, e.g., a collective vibrational state, embedded in the background states in the highly excited nuclei. Keeping in mind the damping mechanism of the giant resonances, we herewith adopt a model system in which the damping of a collective state takes place through coupling to doorway states which consist of only a part of the background states. The strength function of the collective state exhibits not only spreading of the strength common for all damping phenomena but also fine structures reflecting the presence of the doorway states. We shall discuss in detail how the scaling analysis describes characteristics of this kind of strength fluctuations.

#### A. Model

The Hamiltonian of the model is given by

$$H = \omega_c |c\rangle\langle c| + V_{\text{doorway}} + H_{\text{bg}}, \quad (18)$$

where  $|c\rangle$  denotes the collective state, whose energy is  $\omega_c$ . The third term represents the Hamiltonian for the background states, which include the doorway states as well as the other background states. The second term  $V_{\text{doorway}}$  represents the coupling of the collective state  $|c\rangle$  to the doorway states.

Here we keep in mind the picture that shell model many-particle many-hole excitations form basis states  $\{|\mu\rangle\}$  of the background states and the interaction among the basis states causes configuration mixing. As a simplified treatment, we assume that  $H_{\text{bg}}$  has diagonal term representing the unperturbed energies of the basis states, and for the interaction among the basis states we employ a GOE Hamiltonian. Namely,

$$H_{\text{bg}} = \sum_{\mu} \omega_{\mu} |\mu\rangle\langle\mu| + H_{\text{GOE}}, \quad (19)$$

$$H_{\text{GOE}} = \sum_{\mu} v_{\mu\mu}^{\text{d}} |\mu\rangle\langle\mu| + \sum_{\mu>\nu} v_{\mu\nu}^{\text{nd}} (|\mu\rangle\langle\nu| + h.c.). \quad (20)$$

The basis energy  $\omega_{\mu}$  is given by an equidistant model,

$$\omega_{\mu} = \left(-\frac{N_{\text{bg}}}{2} + \mu\right)d \quad (\mu = 1, \dots, N_{\text{bg}}), \quad (21)$$

where  $d$  is the level spacing of the background states and  $N_{\text{bg}}$  represents the total number of backgrounds. Matrix elements  $v_{\mu\mu}^{\text{d}}$  and  $v_{\mu\nu}^{\text{nd}}$  ( $\mu \neq \nu$ ) for the GOE Hamiltonian are independent Gaussian random variables with the zero mean and the variance satisfying  $\langle (v_{\mu\mu}^{\text{d}})^2 \rangle = 2\langle (v_{\mu\nu}^{\text{nd}})^2 \rangle$ . Because of the interaction, the background states have their own spreading width, denoted  $\gamma$  hereafter, which can be estimated as,

$$\gamma = 2\pi \frac{\langle (v_{\mu\nu}^{\text{nd}})^2 \rangle}{d}. \quad (22)$$

The background Hamiltonian (19) is equivalent to the model adopted in ref. [30] and the same as the Wigner ensemble random matrix model [31].

The second term in Eq. (18) representing the coupling between the collective state and doorway states is given by

$$V_{\text{doorway}} = \sum'_{\mu=\text{doorway}} V_{\mu}^{\text{door}} (|c\rangle\langle\mu| + h.c.). \quad (23)$$

Here the interaction is present only for a part of the background  $\mu$  states which are supposed to be the doorway states of the damping, and the summation in Eq.(23) runs only over the doorway states. The doorway  $\mu$  states are selected in every  $L$   $\mu$ -states (i.e.,  $\mu$  states with  $\mu = L, 2L, 3L, \dots$ ). Accordingly, the level spacing of doorway states is  $D = Ld$ . The coupling matrix elements  $V_{\mu}^{\text{door}}$  are random variables taken from a Gaussian distribution with zero mean.

By diagonalizing the Hamiltonian with use of the basis consisting of all the  $\mu$  states and the collective state  $|c\rangle$ , we obtain for each realization of random variables the energy eigenstates  $|i\rangle$ , their energy  $E_i$  and associated strength  $S_i = |\langle c|i\rangle|^2$  of the collective state. The strength function of the collective state

$$S(E) = \sum_i S_i \delta(E - E_i) \quad (24)$$

is thus obtained. Since the collective-doorway couplings are uniform with respect to the energy of the background states, the strength function exhibits as a global profile the Lorentzian distribution. In fact, when we average the strength distribution over many realizations of the Hamiltonian and make smoothing with respect to the energy  $E$ , the averaged strength function  $\tilde{S}(E)$  becomes very close to the Lorentzian whose FWHM is given by the golden rule estimate

$$\Gamma = 2\pi \frac{\langle (V_{\mu}^{\text{door}})^2 \rangle}{D}. \quad (25)$$

In this paper we do not discuss the global spreading profile since it is trivial in this model and it often has simple profile such as Lorentzian also in the experimental data. Instead we deal only with fine structures and fluctuations of the strength function. It is then useful to remove the global smooth profile by normalizing the strength  $S_i$  as

$$\bar{S}_i = \mathcal{N} \frac{S_i \tilde{\rho}(E_i)}{\tilde{S}(E_i)}. \quad (26)$$

Here,  $\tilde{S}(E)$  and  $\tilde{\rho}(E)$  are obtained by averaging the calculated strength function, Eq.(24), and the level density  $\rho(E) = \sum_i \delta(E - E_i)$  over realizations and by smoothing with respect to  $E$  with use of the Gaussian weighting and the Laguerre polynomials as adopted in the Strutinsky method [32].  $\mathcal{N}$  is an overall normalization factor to guarantee  $\sum_i \bar{S}_i = 1$ . As we discussed in connection with the GOE strength fluctuation (Sec. IIB2 and Appendix B), effect of the energy level fluctuation on the fluctuation of the strength function is small except for very small energy scale less than about ten times of the level spacing  $d$ . Furthermore the level fluctuations within a small energy interval is described by the GOE model as far as  $\gamma$  is not small. Thus we neglect the fluctuation of the energy levels in the following analysis. In other words, we use the level order  $i$  as the scale of the excitation energy of the levels instead of the energy  $E_i$  itself. This is equivalent to assume that the energy levels are equidistantly distributed as  $E_i = id$ . In the following, we treat unfolded strength function  $\bar{S}(E) = \sum_i \bar{S}_i \delta(E - E_i)$  thus obtained.

The number of background states is fixed to  $N_{\text{bg}} = 8191$  so that the size of the Hamiltonian matrix has the dimension of 8192. The unperturbed energy of the collective state is placed at the energy center of the spectrum by putting  $\omega_c = 0$ , and we set the FWHM of the global strength distribution  $\Gamma = 2000d$  so that the most of the strengths are located dominantly in the central region of the total spectra. For the interaction matrix elements in  $H_{\text{bg}}$ , or equivalently, the spreading width  $\gamma$  of the background states, we use several different values  $\gamma = 64d, 128d, 256d$ , and  $512d$  to see the dependence on  $\gamma$ . The spacing  $D$  between the doorway states is also varied as  $D = 64d, 128d$ , and  $256d$ , corresponding to the number of doorways 128, 64, 32, respectively.

By generating random numbers for the Gaussian variables in the Hamiltonian, a realization of the Hamiltonian is obtained. The spectra and the strength distribution are calculated for each realization. We perform an average over many realizations of the Hamiltonian to obtain the features which is independent of specific realizations. For this purpose we generate repeatedly the random numbers in  $V_{\text{doorway}}$ , but fix the coefficients in  $H_{\text{bg}}$  ( $H_{\text{GOE}}$ ) since the results do not depend very much on realizations of  $H_{\text{GOE}}$  because of sufficiently large dimension  $N_{\text{bg}}$ . For the ensemble average, we perform averaging over 60 realizations, which is enough to obtain almost exact results for the GOE fluctuations (Sec. IIB2).

The partition function is calculated for the bin widths of powers of 2 of the level spacing  $d$ , i.e.,  $\epsilon = ld$ ,  $l = 1, 2, 4, 8, 16, \dots, 4096$ . Since the number of levels is finite, we need to take care of the edges of the strength distribution. The bins placed at either edge of the spectra have smaller bin width than those in the other part of the spectra, and this would affect the partition function when the bin width is not very small compared to the whole spectrum width. To avoid the edge effect, we assumed a periodic continuation of the spectra by imposing  $\bar{S}_{i+N_{\text{tot}}} = \bar{S}_i$ , where  $N_{\text{tot}}$  is the total number of levels  $N_{\text{tot}} = N_{\text{bg}} + 1$ . For the calculation of the partition function, we performed averaging over 16 bin boundary positions by sliding the bin boundaries by  $l/16$  (we average over  $l$  boundary positions for  $l < 16$ ), which provides sufficient averaging.



An example of the strength function is shown in Fig. 3(a). Qualitatively the distribution looks a Lorentzian distribution as a gross profile. However, the distribution has large fluctuation around the Lorentzian shape. In addition to apparent level-to-level fluctuations, one can recognize clustering of strengths. The latter appears to reflect the distribution of the collective-doorway couplings as seen from the comparison with Fig. 3(b), which shows the strength distribution which is obtained by assuming pure doorway states, i.e., by neglecting the interaction between the doorway states and the other background states. Note however that it is very hard to identify individual doorway states in the strength distribution of Fig. 3(a) since in this example the spreading width of doorway states,  $\gamma$ , is larger than the spacing between the doorways,  $D$ . The strengths associated with individual doorways overlap with each other. Fig. 3(c) shows the distribution of the normalized strength (corresponding to Fig. 3(a)) for which we apply the scaling analysis.

Fig. 4(a) shows the nearest neighbor level spacing distribution (NND) for  $D = 128d$  and  $\gamma = 256d$ . The NND follows the Wigner distribution [8] perfectly, indicating that the fluctuation of the energy level at a short energy interval obeys the GOE random matrix limit. By using the same Hamiltonian as our background Hamiltonian  $H_{\text{bg}}$ , Guhr et al. [30] showed that the GOE limit of the NND is reached as the spreading width of the background states  $\gamma$  becomes larger than several tens of the level spacing  $d$ . Fig. 4(b) shows the statistical distribution of strength  $\bar{S}_i$  of individual level for  $D = 128d$  and  $\gamma = 256d$ . Here the histogram of distribution of square root strength  $\bar{S}_i^{1/2}$  is plotted together with the Porter-Thomas distribution drawn by the dashed curve. Note that the Porter-Thomas distribution  $P(S) = \exp(-S/2)/\sqrt{2\pi S}$  has a Gaussian shape in this plotting. Deviation from the Porter-Thomas distribution is clearly seen. The excess of large and small strengths compared to the Porter-Thomas distribution indicates that the strength fluctuation is larger than the GOE limit. The deviation is caused by the clustering of the strength distribution, which originates from the fine structures of the strength functions associated with doorway states of the damping of the collective state.

## B. Scaling Analysis

### 1. Characteristics of $D_m(\epsilon)$

Let us analyze the strength fluctuation by applying the scaling analysis which we introduced in the previous section.

Figures 5 and 6 display the partition functions  $\chi_m(\epsilon)$  and the local scaling dimensions  $D_m(\epsilon)$ , respectively, for the strength functions calculated with four different values of  $\gamma$  and fixed value of  $D = 128d$ . From the partition function  $\chi_m(\epsilon)$ , one sees that the fluctuation does not follow the power scaling law (or linear relation in the log-log plot). Correspondingly, the local scaling dimension  $D_m(\epsilon)$  varies as a function of  $\epsilon$ . The local scaling dimensions in the four cases show common features. Namely, at small values of  $\epsilon$ ,  $D_m(\epsilon)$  monotonically increases with  $\epsilon$ . As  $\epsilon$  increases further,  $D_m(\epsilon)$  starts to decrease, but it turns to increase again. At the largest value of  $\epsilon$  comparable to the whole spectrum range,  $D_m(\epsilon)$  converges to the uniform limit  $D_m(\epsilon) = 1$ .

Comparing with the local scaling dimension  $D_m(\epsilon)$  for the GOE strength fluctuation indicated with dashed curve in the figure, one sees that the behavior of  $D_m(\epsilon)$  at small  $\epsilon$  follows the GOE limit whereas it deviates from the GOE limit as  $\epsilon$  increases. It is seen that the energy scale  $\epsilon$  where  $D_m(\epsilon)$  starts to deviate from the GOE limit, which we denote  $\epsilon^*$ , has strong correlation to the value of  $\gamma$ . As we discussed in terms of the level spacing distribution, the GOE limit is realized as far as the small energy interval is concerned. However, mixing between the background states (including the doorway states) takes place only within a finite energy interval, that is, the spreading width  $\gamma$  of the background states. Therefore, the fluctuations far below the energy scale  $\gamma$  will obey the GOE limit, while those comparable to or larger than  $\gamma$  may deviate from the GOE limit. In fact, one observes in Fig. 6 that the energy scale  $\epsilon^*$  where  $D_m(\epsilon)$  starts to deviate from the GOE limit is related approximately to  $\gamma$  as  $\epsilon^* \sim 1/5\gamma$ .

Figure 6 also shows clearly that the decrease of  $D_m(\epsilon)$  at the intermediate energy scale  $\epsilon$  depends strongly on the parameter  $\gamma$ . In fact, the value of  $\epsilon$ , denoted  $\epsilon^{**}$ , where  $D_m(\epsilon)$  decreases most sharply corresponds well to the value of  $\gamma$ , indicated by the arrow in the figure, and it moves as one changes  $\gamma$ . Namely  $\epsilon^{**} \sim \gamma$  is observed for all panels in the figure. The close connection between  $\gamma$  and the decrease of  $D_m(\epsilon)$  can be explained as follows. The presence of the doorway states causes the fine structure or the clustering of the strength distribution. When the spreading width  $\gamma$  of the doorway states is small, the doorway states form many peaks (clusters) where width of individual peaks is given by  $\gamma$ . Using the bin width  $\epsilon$  comparable with the spreading width  $\gamma$ , the scaling analysis uncovers the profile of the peaks associated with the doorways. Since the profile will look the Lorentzian shape of width  $\gamma$ , the local scaling dimension  $D_m(\epsilon)$  decreases sharply around  $\epsilon \sim \gamma$  as we found for the smooth Lorentzian distribution (Sec.II B 1). When  $\gamma$  is larger than the spacing  $D$  of the doorway states, the peaks overlap with each other and one cannot trace the individual doorway states. However, the fluctuations of the strength distribution still reflects the spreading width  $\gamma$  of doorway states since the fluctuations associated with the doorway states are not completely smeared out. Thus correspondence between the spreading width  $\gamma$  of doorway states and the point of steepest decrease in  $D_m(\epsilon)$  holds also for the cases of  $\gamma \gtrsim D$ . This situation corresponds to Figs. 6(c) and (d).

The increase of  $D_m(\epsilon)$  at the largest energy scales arises from another features of the doorway states, that is, the fluctuation in the collective-doorway coupling. If we consider only the doorway states and neglect their coupling to other backgrounds, the strengths are concentrated only on the doorway states, as shown in Fig. 3(b). In this limit the strengths of the doorways follow a GOE strength fluctuation, since the collective-doorway coupling matrix elements is chosen as Gaussian random variables. It should be noted that the energy scale associated with this GOE is not the level spacing  $d$  of the whole spectrum, but the spacing  $D$  between the doorways, which is much larger than  $d$ . The dotted curve in Fig. 6 represents the GOE strength fluctuation characterized by the level spacing  $D$  of the doorway states. When the bin width  $\epsilon$  is taken larger than the spreading width  $\gamma$  of the doorway states, the fluctuations at smaller energy scale are smeared out, and only the fluctuation of the collective-doorway coupling remains. In all cases in Fig. 6, the local scaling dimensions follow this curve at the largest energy scales, indicating that the strength fluctuation in this domain reflects the structure of the collective-doorway coupling.

One may also notice that the dip of  $D_m(\epsilon)$  around  $\epsilon \sim \gamma$  becomes small and  $D_m(\epsilon)$  approaches to the GOE limit as one increase the value of  $\gamma$ . It is also noted that for small value of  $\gamma$ , the local scaling dimension  $D_m(\epsilon)$  for the higher moments  $m$  takes significantly smaller value around the intermediate  $\epsilon$  than  $D_m(\epsilon)$  for the lower moments (eg.  $D_5$  vs.  $D_2$ ), while, for large  $\gamma$ ,  $D_m(\epsilon)$  for all moments takes similar value. The higher moments are sensitive to components of the large strength  $p_n$ . Therefore, small value of  $D_m(\epsilon)$  for higher moments implies that the strength distribution is very spiky. In other words the strengths are clustered and form large peaks. On the contrary, similar values of  $D_m(\epsilon)$  close to 1, obtained for large  $\gamma$  values, implies relatively uniform distribution of strengths. The above two features characterize the way how the fine structures (or clustering) associated with the doorway states diminishes as  $\gamma$  increases.

In Fig. 7, we show dependence on the parameter  $D$ , the spacing of the doorway states, with the spreading width  $\gamma$  being kept constant. It is seen that the values of local scaling dimension  $D_m(\epsilon)$  at larger energy scale  $\epsilon$  depends on the spacing  $D$  of doorway states. When  $D$  is small (e.g. Fig. 7(a), where  $D = 64d$ ),  $D_m(\epsilon)$  takes larger value close to the GOE limit than the case of larger  $D$ . This implies that when the strength of each doorway states overlaps significantly with each other, namely, the spacing  $D$  of doorway states is much smaller than spreading width  $\gamma$ , the fluctuation associated with the doorways tends to be smeared. On the other hand, when  $\gamma \lesssim D$ , the fluctuation associated with the doorways stands up clearly, then  $D_m(\epsilon)$  exhibits large deviation from the GOE limit. However, it is more important to note that the spacing  $D$  of the doorways does not affect very much the behavior of  $D_m(\epsilon)$  at smaller energy scale. In both cases of Fig. 7, the values  $\epsilon^*$  and  $\epsilon^{**}$  where  $D_m(\epsilon)$  deviates from the GOE and decreases most sharply, respectively, have relations to  $\gamma$ ,  $\epsilon^* \sim 1/5\gamma$  and  $\epsilon^{**} \sim \gamma$ , as was observed in Fig.6, indicating that these features hold in spite of the change of  $D$  values.

In Fig. 6 we also plot with the dashed-dotted curve  $D_2(\epsilon)$  which is evaluated by means of the exact expression Eq. (34) based on the derivative definition Eq. (6). It is seen that difference between the exact evaluation and the evaluation Eq. (7) based on the finite difference is almost indistinguishable. This justifies the use of the finite difference evaluation of the local scaling dimension.

## 2. $D_m(\epsilon)$ as a measure of doorway spreading width

The close relation between the spreading width  $\gamma$  and the profile of the local scaling dimension may be used as a tool to estimate the spreading width  $\gamma$  of the doorway states. The number of doorway states which are involved in the damped collective states such as the giant resonances is not small. In such cases, it is difficult to evaluate the spreading width by distinguishing individual doorway states from the whole strength distribution since the strengths associated with each doorway states may overlap with each other. On the other hand, since the scaling analysis discussed in this paper does not assume separation of the peaks, it is applicable in such overlapping cases. Indeed, the numerical analysis presented above indicates that the characteristic behavior of  $D_m(\epsilon)$ , namely the decrease around the energy scale comparable with  $\gamma$ , shows up even in cases where the spreading width  $\gamma$  is larger than the spacing  $D$  between the doorway states. Thus one may estimate the spreading width  $\gamma$  by locating the point  $\epsilon^{**}$  where  $D_m(\epsilon)$  decreases most steeply.

It is instructive to compare with the autocorrelation analysis, which is often used to analyze the strength fluctuations. As discussed in the previous section, there is the relation between the autocorrelation analysis and the scaling analysis, in particular, between the autocorrelation function  $C_2(\epsilon)$  and the local scaling dimension  $D_2(\epsilon)$  for the second moment. Figure 8 shows the autocorrelation function  $C_2(\epsilon)$  for  $D = 128d$  and  $\gamma = 256d$ , which is also calculated for the normalized strength distribution (e.g. Fig. 3(c)) and averaged over 60 realizations as done for the scaling analysis. The autocorrelation function  $C_2(\epsilon)$  exhibits the following property. It has a broad peak centered around  $\epsilon = 0$  which is built upon a flat ‘background’. The broad peak contains the information of the fine structure of the strength fluctuations which arises from the doorway states. The width of the broad peak corresponds well to the spreading

width  $\gamma$  of the doorway states. It is helpful to remind that the autocorrelation function used to analyze the Ericson fluctuation in cross sections of highly excited compound nuclei, where resonance overlaps with neighboring ones. In that case, the width of the autocorrelation function is related to the particle decay width of individual states. In our case, on the other hand, the width of the autocorrelation function is related to the spreading width of the doorway states. Comparing Fig. 6 and Fig. 8, one sees close relationship between the local scaling dimension  $D_2(\epsilon)$  and the autocorrelation function  $C_2(\epsilon)$ , both of which decrease sharply at the energy scale corresponding to  $\gamma$ .

### 3. Analysis without ensemble average

The results presented above are obtained by averaging over sixty different strength functions which are calculated for every realization of the random Hamiltonian. This is possible for the model systems. However, there will be a situation where one has only a single experimental data for a given nucleus so that one cannot perform ensemble average. When one applies the scaling analysis to a single given spectrum, the result will contain both the property which is common for the ensemble which the data belongs to and the behavior which is specific to the given realization of spectra. The latter can be regarded as fluctuation associated with different realizations. The fluctuation indicates an uncertainty when we infer the ensemble averaged properties from analysis of a single spectrum. To evaluate this uncertainty in the local scaling dimension  $D_m(\epsilon)$ , we calculate the local scaling dimensions  $D_m(\epsilon)$  for each of 60 realizations of the model Hamiltonian, and evaluate the average and the standard deviation in  $D_m(\epsilon)$ . The results are plotted in Fig. 9. We also plot in the same figure an example of  $D_m(\epsilon)$  for an arbitrarily chosen realization.

It is seen that the local scaling dimension calculated for a single realization shows  $\epsilon$  dependence which is qualitatively same as the ensemble averaged  $D_m(\epsilon)$ . The standard deviation from the average is smaller than the typical size of  $\epsilon$  dependence of  $D_m(\epsilon)$  for the cases shown in the figure. It is seen that the deviation increases as  $m$  increases, namely, as the higher moments are concerned. The standard deviation in  $D_m(\epsilon)$  is estimated approximately as  $\sigma(D_m) \approx \sqrt{3m}/\sqrt{N_{\text{tot}}}$  by assuming independent Porter-Thomas fluctuation for the individual strengths  $S_i$ . Thus, the local scaling dimensions  $D_m(\epsilon)$  calculated for a single data are not affected very much by the fluctuation due to the realizations and keep information on the background mechanisms such as the spreading width  $\gamma$  of the doorway states as far as a sufficient number of levels are included in the analysis and the low order moments are concerned.

## IV. Conclusions

We proposed a new method to analyze fluctuation properties of the strength functions by means of the scaling analysis similar to the multifractal analysis. In order to treat the non-scaling fluctuations, we introduced the local scaling dimension  $D_m(\epsilon)$  defined as a function of a scaling parameter  $\epsilon$ , which is the energy bin width subdividing the strength function. This quantity reduces to the generalized fractal dimension if a self-similar structure exists in the strength fluctuation. The local scaling dimension also has a close connection with the autocorrelation function of the strength function.

Strength functions associated with damped excited modes such as the giant resonances may exhibit various fluctuations and fine structures arising from different mechanisms including the doorway structures of damping and the Porter-Thomas or GOE strength fluctuations associated with individual levels. Employing a model which mimics the doorway damping of the giant resonances, we applied the method to analyze the strength fluctuations associated with the doorway structures. The close relation between the profile of the local scaling dimension and the fluctuations embedded in the strength function is studied in detail. We showed that the behavior of the local scaling dimension  $D_m(\epsilon)$  as a function of the binning energy scale  $\epsilon$  manifests clearly both the GOE fluctuation at the small energy scale and the properties associated with the doorway states. For example, the binning energy scale  $\epsilon^{**}$  where the local scaling dimension  $D_m(\epsilon)$  decreases sharply corresponds to the spreading width  $\gamma$  of the doorway states. This demonstrates that the local scaling dimension can be an useful measure to analyze the fluctuations and fine structures of the strength function associated with the damping modes in highly excited nuclei.

It is in principle possible to apply the scaling analysis discussed in the paper to the experimental spectra and also to strength functions in realistic descriptions of the giant resonances in order to study the mechanism responsible for the strength fluctuations, such as the spreading width of the doorway states. The method itself is, on the other hand, quite general and not restricted to the giant resonances, and applicable to any strength fluctuation phenomenon in nuclei as well as in the other fields of quantum physics.

## ACKNOWLEDGMENTS

The authors acknowledge helpful discussions with Kenichi Matsuyanagi, Toru Suzuki, and Shoujirou Mizutori. The numerical calculations are performed at the Yukawa Institute Computer Facility. The work is supported by the Grant-in-Aid for Scientific Research from the Ministry of Education, Science and Culture (No. 10640267).

### A. Explicit Expression of Partition Function and Local Scaling Dimension

We derive here an explicit expression of  $\chi_m(\epsilon)$  given in terms of the strength  $S_i$  and the energy  $E_i$  of individual levels.

The quantity  $p_n$  defined in Eq. (2) can be written as

$$p_n = \sum_i S_i \theta_n(E_i), \quad (27)$$

by using a step function

$$\theta_n(x) \equiv \begin{cases} 1 & \text{for } x \text{ in } n\text{-th bin} \\ 0 & \text{for } x \text{ not in } n\text{-th bin.} \end{cases} \quad (28)$$

Then, the partition function is also rewritten as

$$\chi_m(\epsilon) = \sum_{i_1, \dots, i_m} S_{i_1} \cdots S_{i_m} \langle \sum_n \theta_n(E_{i_1}) \cdots \theta_n(E_{i_m}) \rangle_{\text{bin}}, \quad (29)$$

where  $\langle \cdots \rangle_{\text{bin}}$  represents an average with respect to the bin boundary as explained in Sec. II A. The quantity  $\sum_n \theta_n(E_{i_1}) \cdots \theta_n(E_{i_m})$  takes the value of either 1 or 0. Denoting the difference between the largest value and the smallest value among  $E_{i_1}, \dots, E_{i_m}$  by  $D_{i_1 \dots i_m}$ , the probability of the quantity being 1 is evaluated as  $(\epsilon - D_{i_1 \dots i_m})/\epsilon$ . In addition, the quantity  $\langle \cdots \rangle_{\text{bin}}$  should be zero if  $D_{i_1 \dots i_m}$  is larger than the bin width  $\epsilon$ . Thus,  $\chi_m(\epsilon)$  can be calculated as

$$\chi_m(\epsilon) = \sum_{i_1, \dots, i_m} S_{i_1} \cdots S_{i_m} \theta(\epsilon - D_{i_1 \dots i_m}) \frac{\epsilon - D_{i_1 \dots i_m}}{\epsilon}, \quad (30)$$

$$\theta(x) \equiv \begin{cases} 1 & x > 0 \\ 0 & x \leq 0. \end{cases} \quad (31)$$

As a result, the local scaling dimension  $D_m(\epsilon)$  can be explicitly written as

$$D_m(\epsilon) = \frac{\sum_{i_1, \dots, i_m} S_{i_1} \cdots S_{i_m} \theta(\epsilon - D_{i_1 \dots i_m}) D_{i_1 \dots i_m}}{\sum_{i_1, \dots, i_m} S_{i_1} \cdots S_{i_m} \theta(\epsilon - D_{i_1 \dots i_m}) (\epsilon - D_{i_1 \dots i_m})}. \quad (32)$$

In particular, for the case of  $m = 2$ , Eq. (30) and Eq. (32) lead to

$$\chi_2(\epsilon) = \sum_{ij} S_i S_j \theta(\epsilon - |E_i - E_j|) \frac{\epsilon - |E_i - E_j|}{\epsilon}, \quad (33)$$

and

$$D_2(\epsilon) = \frac{\sum_{ij} S_i S_j \theta(\epsilon - |E_i - E_j|) |E_i - E_j|}{\sum_{ij} S_i S_j \theta(\epsilon - |E_i - E_j|) (\epsilon - |E_i - E_j|)}, \quad (34)$$

respectively.

## B. Local Scaling Dimensions for GOE Strength Fluctuations

The local scaling dimension associated with the GOE strength fluctuation can be calculated as follows under the assumption that the energy levels are equally spaced  $E_i = id$  ( $i = 1, 2, \dots, N_{\text{tot}}$ ). Since the strength  $S_i$  of  $i$ -th level is written as  $S_i = x_i^2$  in terms of amplitudes  $x_i$  which obeys the GOE amplitude distribution with dimension  $N_{\text{tot}}$  [8]

$$P_{\text{GOE}}(x_1, \dots, x_{N_{\text{tot}}}) = \pi^{-\frac{N_{\text{tot}}}{2}} \Gamma\left(\frac{N_{\text{tot}}}{2}\right) \delta\left(1 - \sum_{i=1}^{N_{\text{tot}}} x_i^2\right), \quad (35)$$

the probability distribution of  $\{p_n\}$  defined by Eq. (2) can be written as

$$f(p_1, \dots, p_L) = \int \dots \int dx_1 \dots dx_{N_{\text{tot}}} \delta\left(p_1 - \sum_{i \in \text{1st bin}} x_i^2\right) \dots \delta\left(p_L - \sum_{i \in L\text{-th bin}} x_i^2\right) P_{\text{GOE}}(x_1, \dots, x_{N_{\text{tot}}}). \quad (36)$$

Considering the case where the bin width  $\epsilon = ld$  ( $l$  being even integer), that is, each bin contains  $l$  levels, and using the variable  $l$  as the scaling parameter instead of  $\epsilon$ , the ensemble average of the partition function can be calculated as

$$\begin{aligned} \overline{\chi_m(l)} &= \int \dots \int dp_1 \dots dp_L \sum_{n=1}^L p_n^m f(p_1, \dots, p_L) \\ &= \frac{N_{\text{tot}}}{l} \frac{\Gamma\left(\frac{N_{\text{tot}}}{2}\right) \Gamma\left(\frac{1}{2}(2m+l)\right)}{\Gamma\left(\frac{1}{2}\right) \Gamma\left(\frac{1}{2}(N_{\text{tot}}+2m)\right)}. \end{aligned} \quad (37)$$

Thus, the local scaling dimension derived from Eq. (7) reads

$$D_m(\sqrt{2}l) = \frac{1}{(m-1)\log 2} \left( -\log 2 + \sum_{i=l}^{m+l-1} \log i - \sum_{i=l/2}^{m+l/2-1} \log i \right). \quad (38)$$

If we use Eq. (6) by taking  $l$  as a continuous variable, the local scaling dimension can be written as

$$D_m(l) = \frac{1}{m-1} \sum_{i=1}^{m-1} \frac{l}{l+2i}. \quad (39)$$

As is seen from Eqs. (38) and (39), the local scaling dimension for the GOE strength fluctuation is independent of the matrix dimension. In deriving the above results, we did not perform an average with respect to the bin boundary for the partition function. This is not necessary since the ensemble average has the same effect for the case of GOE.

In the above evaluation we neglected the fluctuation of the energy levels. The analytic expression which includes both the strength and the energy level fluctuations can be derived for the local scaling dimension of the second moment,  $D_2(\epsilon)$ .

Using Eq. (33), we write the partition function as

$$\epsilon \chi_2(\epsilon) = \int d\epsilon' \int d\epsilon'' \theta(\epsilon - |\epsilon' - \epsilon''|) (\epsilon - |\epsilon' - \epsilon''|) A(\epsilon', \epsilon''), \quad (40)$$

where the function  $A(\epsilon', \epsilon'')$  is defined by

$$A(\epsilon', \epsilon'') \equiv \sum_{ij} S_i S_j \delta(\epsilon' - E_i) \delta(\epsilon'' - E_j). \quad (41)$$

Now, we consider the ensemble average of the function  $A(\epsilon', \epsilon'')$ . Since strengths and energies can be averaged independently, and the average of  $S_i^2$  and that of  $S_i S_j$  ( $i \neq j$ ) do not depend on  $i$  and  $j$ , the result of ensemble average is given by

$$\overline{A(\epsilon', \epsilon'')} = \overline{S_i^2} \delta(\epsilon' - \epsilon'') \sum_i \delta(\epsilon' - E_i) + \overline{S_i S_j} \sum_{i \neq j} \delta(\epsilon' - E_i) \delta(\epsilon'' - E_j). \quad (42)$$

Since the average level density is normalized (unfolded),

$$\overline{\sum_i \delta(\epsilon' - E_i)} = 1, \quad (43)$$

and using the Dyson's two-point cluster function [8,13],

$$\overline{\sum_{i \neq j} \delta(\epsilon' - E_i) \delta(\epsilon'' - E_j)} = 1 - Y(\epsilon' - \epsilon''), \quad (44)$$

the ensemble average of Eq. (40) can be written as,

$$\overline{\epsilon \chi_2(\epsilon)} / N_{\text{tot}} = \overline{S_i^2} \epsilon + \overline{S_i S_j} (\epsilon^2 - \int_{-\epsilon}^{\epsilon} dx (\epsilon - |x|) Y(x)). \quad (45)$$

For the GOE with large  $N_{\text{tot}}$  limit, we have [8,13]

$$\overline{S_i^2} = \alpha \overline{S_i S_j} \quad (\alpha = 3), \quad (46)$$

and

$$Y(\epsilon) = S(\epsilon)^2 - J(\epsilon)D(\epsilon), \quad (47)$$

where the functions  $S(\epsilon)$ ,  $J(\epsilon)$ , and  $D(\epsilon)$  are given by

$$S(\epsilon) \equiv \frac{\sin(\pi\epsilon)}{\pi\epsilon}, \quad (48)$$

$$D(\epsilon) \equiv \frac{dS(\epsilon)}{d\epsilon}, \quad (49)$$

$$J(\epsilon) \equiv \int_0^{\epsilon} d\epsilon' S(\epsilon') - \frac{1}{2} \text{sgn}(\epsilon). \quad (50)$$

Using (45)-(50), the local scaling dimension for the GOE strength fluctuation results in

$$D_2(\epsilon) = \frac{G(\epsilon)}{F(\epsilon)}, \quad (51)$$

where

$$G(\epsilon) = \epsilon^2 - \frac{\sin(\pi\epsilon)}{\pi} (1 + \frac{2}{\pi} \text{Si}(\pi\epsilon)) + \frac{\text{Si}(\pi\epsilon)}{\pi} (1 - \frac{\text{Si}(\pi\epsilon)}{\pi}) + \frac{4}{\pi^2} \int_0^{\pi\epsilon} \cos y \text{Si} y dy, \quad (52)$$

$$F(\epsilon) = \epsilon(\epsilon + \alpha + 1) + \frac{\text{Si}(\pi\epsilon)}{\pi} (\frac{\text{Si}(\pi\epsilon)}{\pi} + \frac{4}{\pi} \sin(\pi\epsilon)) - \frac{4\epsilon}{\pi} (\text{Si}(2\pi\epsilon) - \frac{\sin^2(\pi\epsilon)}{\pi\epsilon}) - \frac{4}{\pi^2} \int_0^{\pi\epsilon} \cos y \text{Si} y dy, \quad (53)$$

$$\text{Si} x \equiv \int_0^x \frac{\sin y}{y} dy. \quad (54)$$

One sees that when  $\epsilon$  is sufficiently larger than the level spacing, or practically when  $\epsilon \gtrsim 10$ , Eq. (51) leads to

$$D_2(\epsilon) \simeq \frac{\epsilon}{\epsilon + \alpha - 1}, \quad (55)$$

which is the same as Eq. (39) with  $m = 2$ . This indicates that the fluctuation of energy levels does not affect the local scaling dimension for  $\epsilon$  which is larger than ten times of level spacing. Note that the effect of the energy level fluctuation on  $D_2(\epsilon)$  is not very large also for the region  $1 < \epsilon < 10$ . At  $\epsilon = 4$ , Eq. (55) gives  $D_2 = 0.67$  while inclusion of the level fluctuation (Eq. (51)) leads to  $D_2 = 0.62$ .

Equation (45) can be used also for the Poisson fluctuation, for which the strength is constant  $\overline{S_i^2} = \overline{S_i S_j}$ , and there is no correlation among energy levels  $Y(x) = 0$ . Then, Eq.(45) leads to, up to a constant factor,

$$\overline{\chi_2(\epsilon)} = \epsilon + 1, \quad (56)$$

and the local scaling dimension  $D_2(\epsilon)$  for the second moment is given by

$$D_2(\epsilon) = \frac{\epsilon}{\epsilon + 1}, \quad (57)$$

which is equivalent to Eq. (10) with  $m = 2$ .

---

- [1] G.F. Bertsch, P.F. Bortignon, and R.A. Broglia, *Rev. Mod. Phys.* **55**, 287 (1983).
- [2] A. van der Woude, *Electric and Magnetic Giant Resonances in Nuclei*, (World Scientific, 1991), p.100.
- [3] P.G. Hansen, B. Jonson, and A. Richter, *Nucl. Phys.* **A 518**, 13 (1990).
- [4] G. Kühner *et al.*, *Phys. Lett.* **B104**, 189 (1981).
- [5] G. Kilgus *et al.*, *Z. Phys.* **A326**, 41 (1987).
- [6] S. Kamedzhiev *et al.*, *Phys. Rev.* **C55**, 2101 (1997).
- [7] C.E. Porter and R.G. Thomas, *Phys. Rev.* **104**, 483 (1956).
- [8] T.A. Brody *et al.*, *Rev. Mod. Phys.* **53**, 385 (1981).
- [9] T. Ericson, *Phys. Rev. Lett.* **5**, 430 (1960); *Annal. Phys.* **23**, 390 (1963);  
T. Ericson and T. Mayer-Kuckuk, *Ann. Rev. Nucl. Sci.* **16**, 183 (1966).
- [10] O. Bohigas and H. Weidenmüller, *Ann. Rev. Nucl. Part. Sci.* **38**, 421 (1988).
- [11] F.J. Dyson, *J. Math. Phys.* **3**, 140, 157, 166 (1962).
- [12] M.L. Mehta, *Random matrices*, 2nd et. (Academic Press, 1991).
- [13] O. Bohigas and M.-J. Giannoni, in *Lecture Notes in Physics 219* (Springer, 1984) 1.
- [14] J.C. Hardy, B. Jonson, P.G. Hansen, *Nucl. Phys.* **A305**, 15 (1978).
- [15] J.L. McCauly, *Chaos, Dynamics and Fractals* (Cambridge University Press, 1993).
- [16] J.L. McCauly, *Phys. Rep.* **189**, 225 (1990).
- [17] J. Feder, *Fractals*(Plenum Press, 1988).
- [18] H. Aoki, *J. Phys.* **C16**, L205 (1983); *Phys. Rev.* **B33**, 7310 (1986).
- [19] C. Castellani and L. Peliti, *J. Phys.* **A19**, L429 (1986).
- [20] M. Janssen, *Phys. Rep.* **295**, 1 (1998).
- [21] H. Aiba, S. Mizutori, and T. Suzuki, *Phys. Rev.* **E56**, 119 (1997).
- [22] A.Z. Górski and S. Drożdż, *Acta Phys. Pol.* **B28**, 1111 (1997).
- [23] H.G.E. Hentschel and I. Procaccia, *Physica* **8D**, 435 (1983).
- [24] T.C. Halsey *et al.*, *Phys. Rev.* **A33**, 1141 (1986).
- [25] L. Leviander *et al.*, *Phys. Rev. Lett.* **56**, 2449 (1986).
- [26] J. Wilkie and P. Brumer, *Phys. Rev. Lett.* **67**, 1185 (1991)
- [27] M. Lombardi and T.H. Seligman, *Phys. Rev.* **A47**, 3571 (1993).
- [28] Y. Alhassid and N. Whelan, *Phys. Rev. Lett.* **70**, 572 (1993).
- [29] A. Bohr and B.R. Mottelson, *Nuclear Structure* (Benjamin, New York, 1996), Vol.1, Chap.2D.
- [30] T. Guhr and H.A. Weidenmüller, *Annal. Phys.* **193**, 472 (1989).
- [31] E.P. Wigner, *Ann. Math.* **62**, 548 (1955).
- [32] P. Ring and P. Schuck, *The Nuclear Many-Body Problem* (Springer, New York, 1980), Chap.2.9.

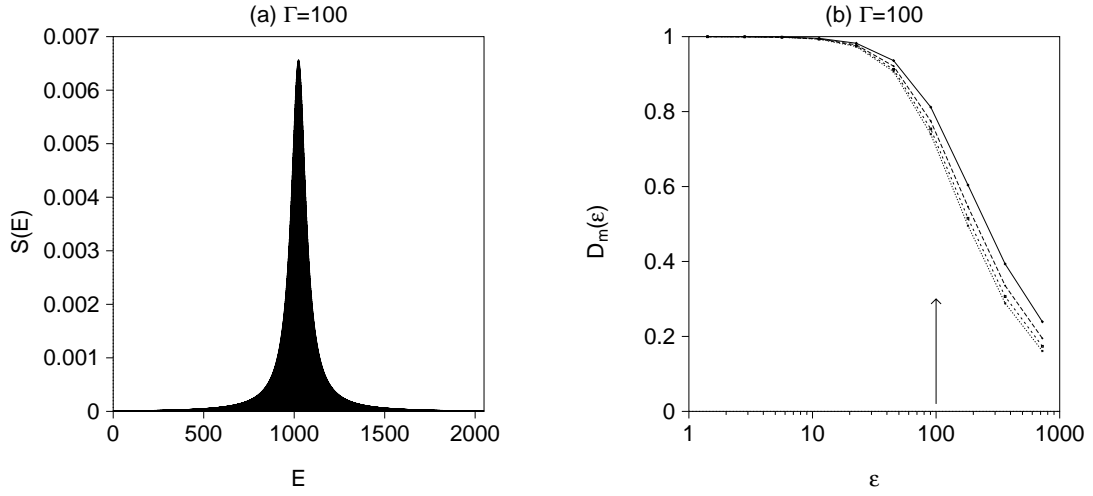


FIG. 1. (a)The Lorentzian strength function, and (b) the corresponding local scaling dimension  $D_m(\epsilon)$ . The curves correspond to  $D_m(\epsilon)$  for  $m = 2$  to  $5$  from upper to lower. The arrow indicates the value of the width  $\Gamma$  of the Lorentzian.

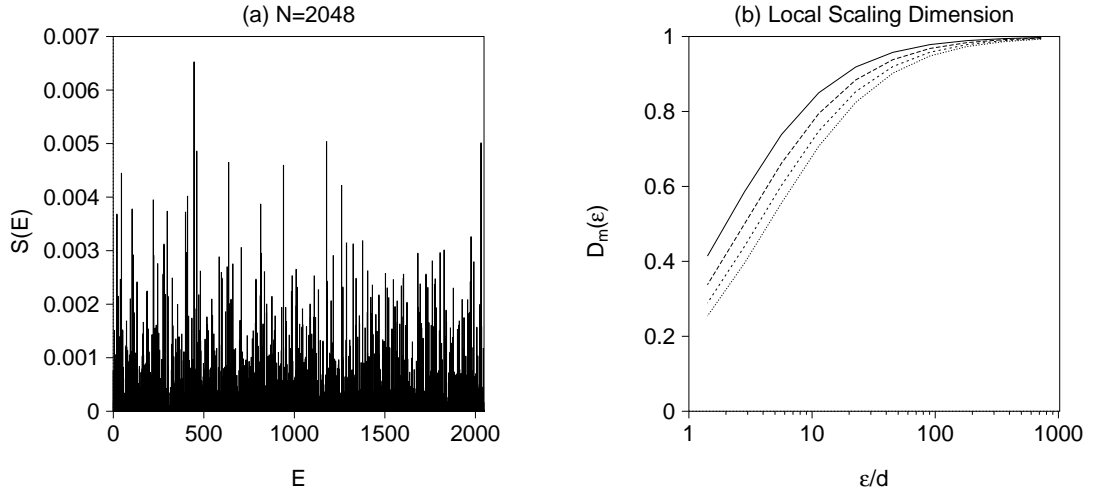


FIG. 2. (a)An example of the GOE strength function with matrix dimension of 2048. (b)The local scaling dimension  $D_m(\epsilon)$  for the GOE strength function obtained after the ensemble average.



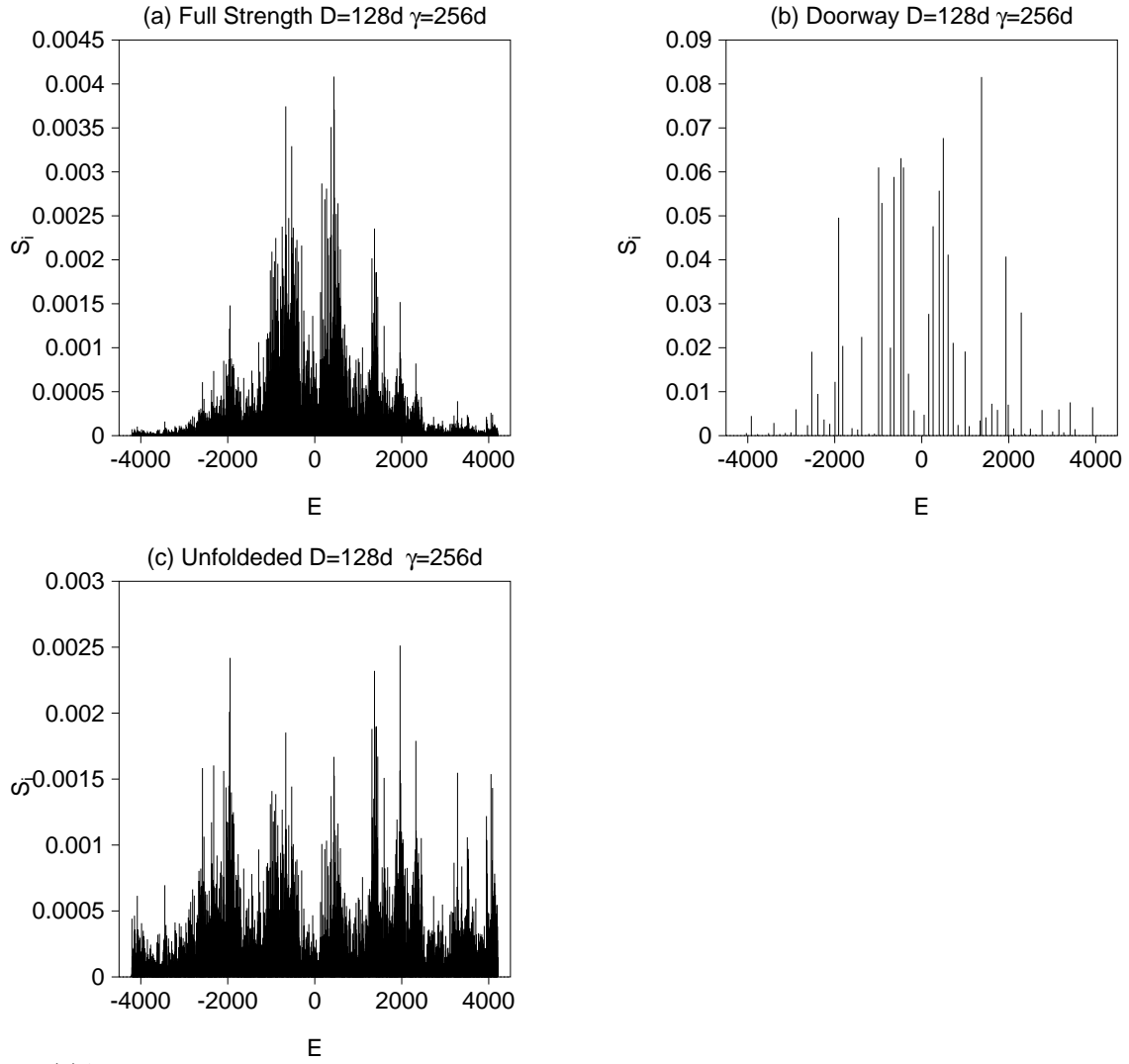


FIG. 3. (a) An example of the strength function obtained in the doorway damping model with parameters  $D = 128d$  and  $\gamma = 256d$ . (b) The same as (a), but coupling between the doorway states and the other background states is neglected. (c) The unfolded strength function  $\bar{S}(E)$  corresponding to the original one plotted in (a).

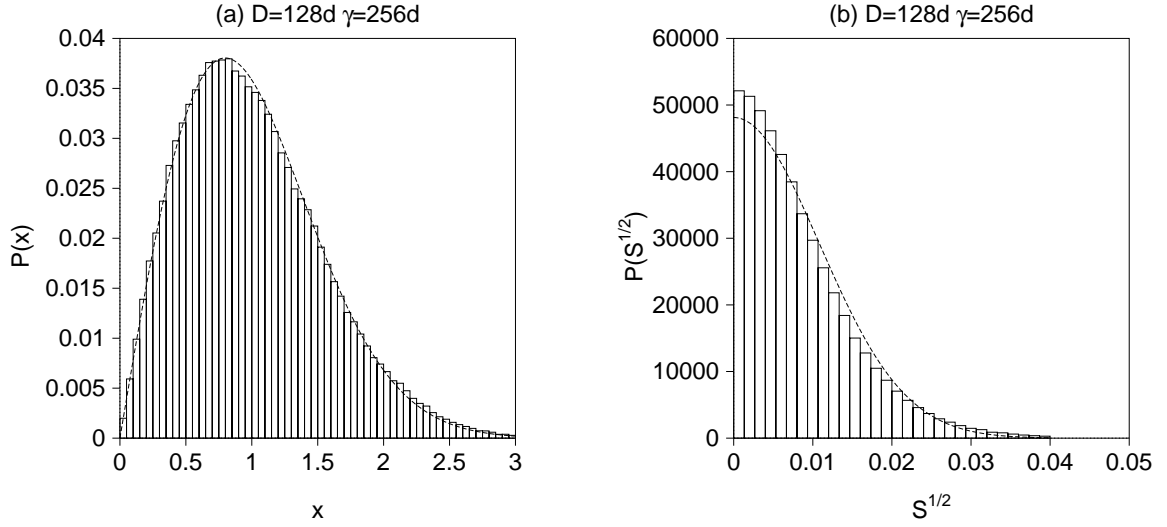


FIG. 4. (a) The nearest neighbor level spacing distribution for the doorway damping model with parameters  $D = 128d$  and  $\gamma = 256d$ . Level spacings were unfolded. The dashed curve represents the Wigner distribution. (b) The statistical distribution of square root of unfolded strengths,  $\bar{S}_i^{1/2}$ , associated with the individual levels for  $D = 128d$  and  $\gamma = 256d$ . The dashed curve represents the Porter-Thomas distribution which becomes a Gaussian when plotted as a function of  $\bar{S}_i^{1/2}$ . Both results are obtained with the ensemble average over 60 realizations of the doorway couplings.

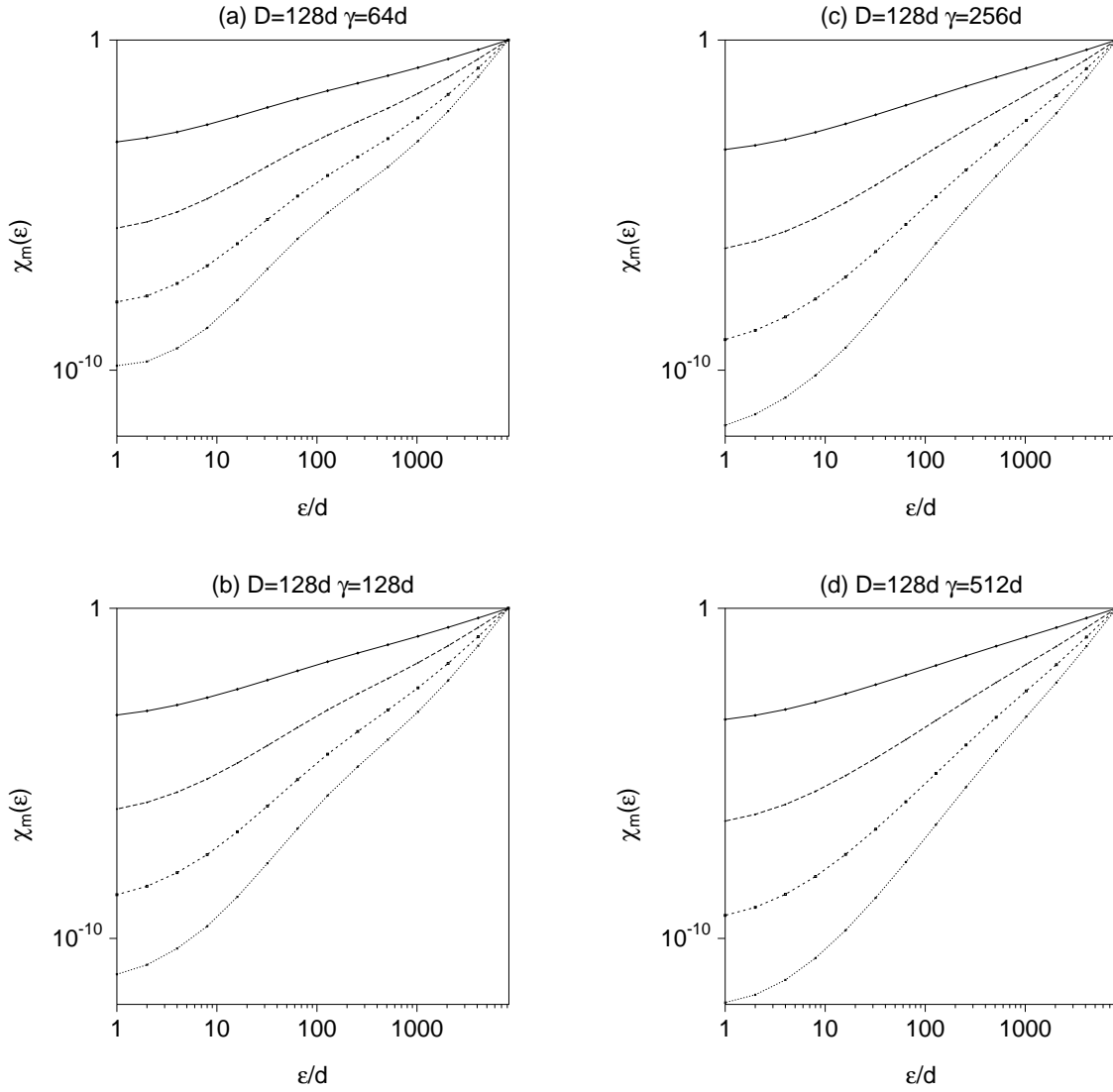


FIG. 5. The partition function  $\chi_m(\epsilon)$  for the doorway damping model with four different values of (a)  $\gamma = 64d$ , (b)  $128d$ , (c)  $256d$ , and (d)  $512d$  while  $D = 128d$  is fixed. The result is obtained with the ensemble average over 60 realizations of the doorway couplings.

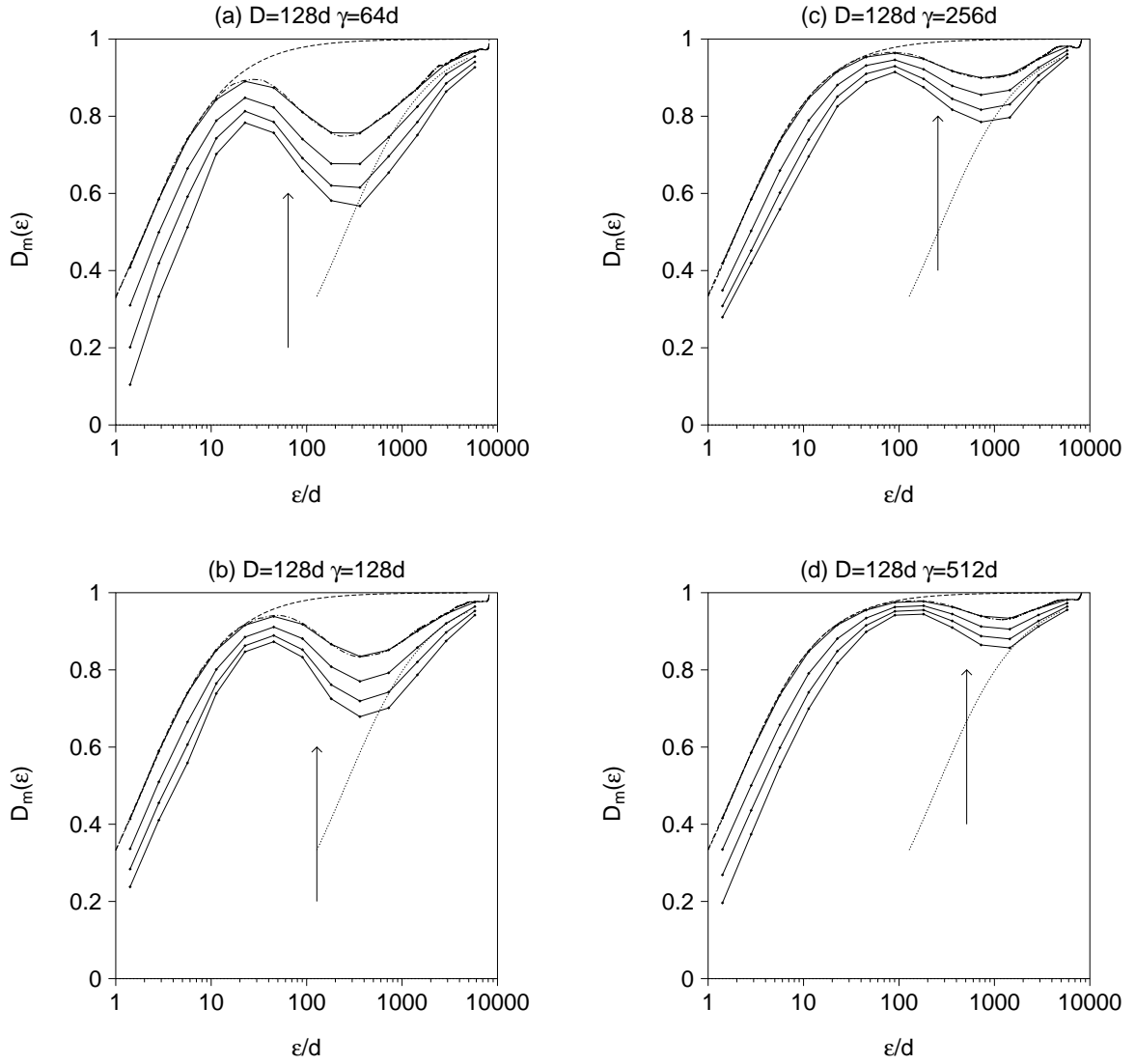


FIG. 6. The local scaling dimension  $D_m(\epsilon)$  for the doorway damping model, corresponding to the partition functions plotted in Fig. 5. The arrows indicate the value of  $\gamma$ , which is chosen as (a)  $\gamma = 64d$ , (b)  $128d$ , (c)  $256d$ , and (d)  $512d$ . The dashed curve represents  $D_2(\epsilon)$  for the GOE. The dotted curve represents the fluctuation associated with the doorway coupling, which is taken the same as a GOE fluctuation with level spacing  $D$  in the present model (see text). The dashed-dotted curve is  $D_2(\epsilon)$  evaluated by using the derivative definition Eqs. (6) and (34) instead of the finite difference.

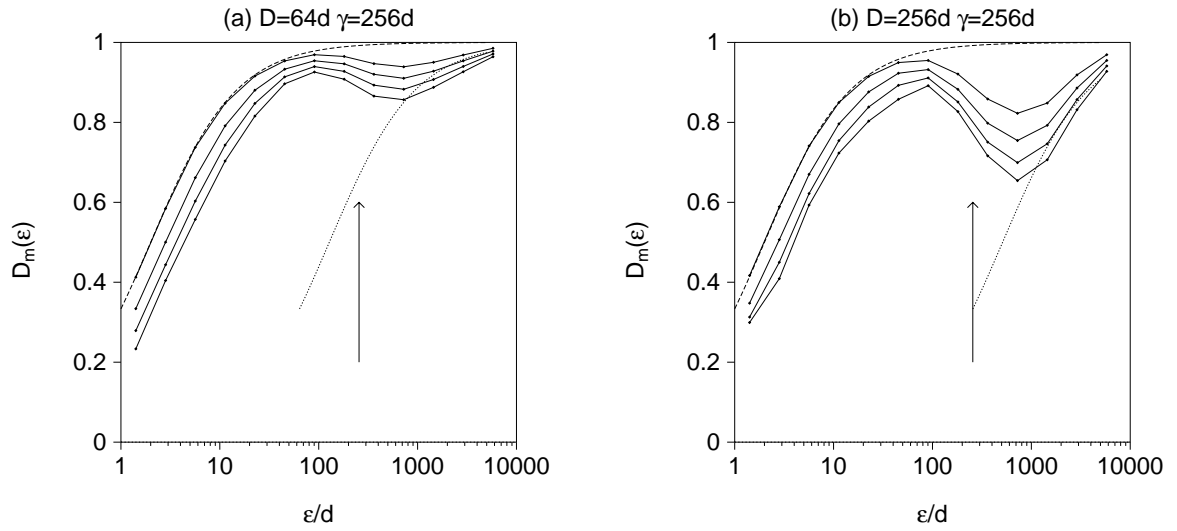


FIG. 7. The same as Fig. 6 but for (a)  $D = 64d$  and  $\gamma = 256d$ , and (b)  $D = 256d$  and  $\gamma = 256d$ .

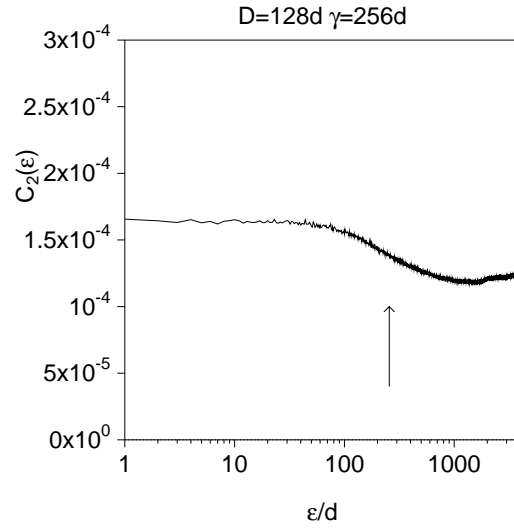


FIG. 8. The autocorrelation function  $C_2(\epsilon)$  of the strength functions for the doorway damping model with  $D = 128d$  and  $\gamma = 256d$ , corresponding to Fig. 6(c). The ensemble average is performed. The arrow indicates the value of  $\gamma$ .

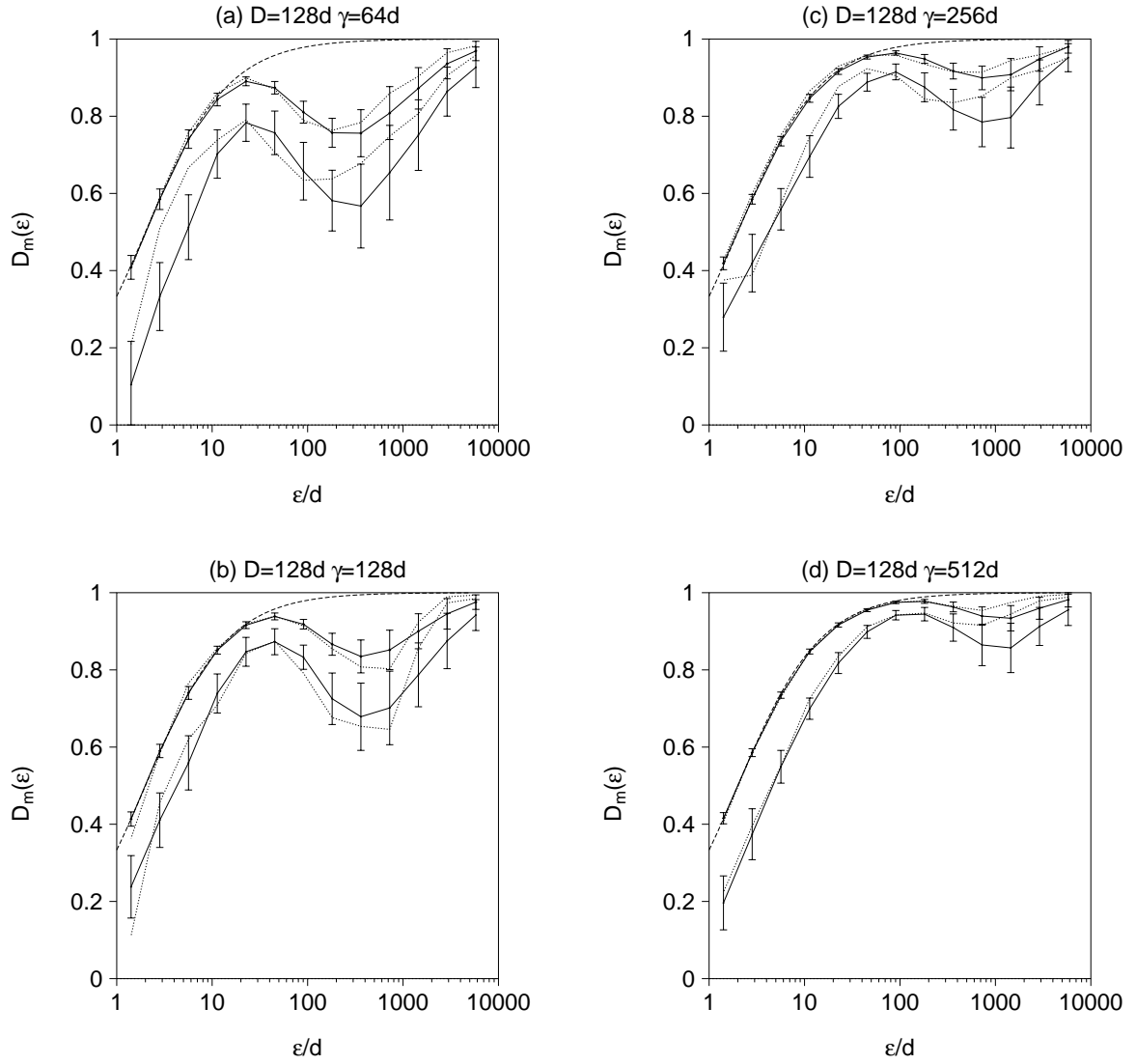


FIG. 9. Comparison of the local scaling dimensions  $D_2(\epsilon)$  and  $D_5(\epsilon)$  between the results obtained with the ensemble average (solid curve) and those for a single realization of spectra (dotted curve), for  $D = 128d$  and (a)  $\gamma = 64d$ , (b)  $128d$ , (c)  $256d$ , and (d)  $512d$ . The bars indicate the standard deviation of  $D_2(\epsilon)$  and  $D_5(\epsilon)$  associated with different realizations, which is evaluated by using the ensemble of the 60 spectra.